DERIVING WINDS FROM POLAR ORBITING SATELLITE DATA

David Santek[1], Jeffrey R. Key[2], Christopher S. Velden[1], Niels Bormann[3], Jean-Noël Thépaut[3], and W. Paul Menzel[2]

[1]Cooperative Institute for Meteorological Satellite Studies, University of Wisconsin-Madison
1225 West Dayton Street, Madison, Wisconsin, USA

[2]Office of Research and Applications, NOAA/NESDIS
1225 West Dayton Street, Madison, Wisconsin, 53706, USA

[3]European Centre for Medium Range Weather Forecasts,
Shinfield Park, Reading, Berkshire, U.K.

ABSTRACT

Wind products from geostationary satellites have been generated for over 20 years, and are used in numerical weather prediction systems. However, because geostationary satellites do not provide useful wind information poleward of the midlatitudes, and because the high-latitude rawinsonde network is sparse, the polar regions remain data poor. This study demonstrates the feasibility of deriving tropospheric wind information at high latitudes from polar-orbiting satellites. The methodology employed is based on the algorithms currently used with geostationary satellites, modified for use with the Moderate Resolution Imaging Spectroradiometer (MODIS). The project presents some unique challenges, including the irregularity of temporal sampling, different viewing geometries in successive orbits, uncertainties in wind vector height assignment as a result of low atmospheric water vapor amounts and thin clouds typical of the Arctic and Antarctic, and the complexity of surface features. A 30-day case study dataset has been produced and is being used in model impact studies. Preliminary results are encouraging: when the MODIS winds are assimilated in the European Centre for Medium Range Weather Forecasts (ECMWF) model, the forecasts of geopotential height for the Arctic and the Northern Hemisphere are improved significantly.

1. Introduction

In the early 1960s, Tetsuya Fujita developed analysis techniques to use cloud pictures from the first TIROS polar orbiting satellite for estimating the velocity of tropospheric winds (Menzel, 2001). Throughout the 1970s and early 1980s, cloud motion winds were produced from geostationary satellite data using a combination of automated and manual techniques. In 1992, the National Oceanic and Atmospheric Administration (NOAA) began using an experimental automated winds software package developed at the University of Wisconsin Space Science and Engineering Center that made it possible to produce a full-disk wind set without manual intervention. The carbon dioxide (CO_2) slicing algorithm (Menzel et al., 1983) made it possible to assign more accurate cloud heights to the motion vectors. Fully automated cloud-drift and water vapor motion vector production from the Geostationary Operational Environmental Satellites (GOES) became operational in 1996, and now wind vectors are routinely used in operational numerical models of the National Centers for Environmental Prediction (NCEP) (Nieman et al., 1997).

Satellite-derived wind fields are most valuable over the oceanic regions where few observations exist and numerical weather prediction model forecasts are less accurate as a result. Like the oceans at lower latitudes, the polar regions also suffer from a lack of observational data. Figure 1 illustrates the sparse observation network in the Arctic and Antarctic. World Meteorological Organization (WMO)

stations, which provide regular wind observations from rawinsondes, are scattered across the coastal areas and the interior of Canada, Alaska, Russia, and northern Europe. However, there is little or no coverage of the interior of Greenland, the interior of Antarctica, the Arctic Ocean, and the oceans surrounding Antarctica.

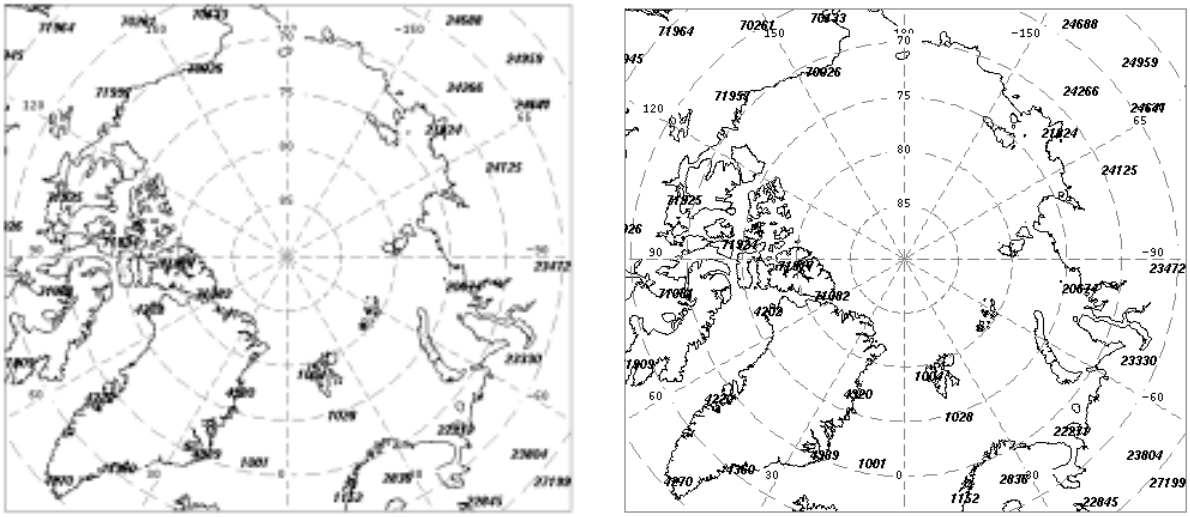

Fig. 1. WMO stations across the Arctic (left) and Antarctic (right). Only those stations that provide regular daily wind data are shown.

Unfortunately, geostationary satellites are of little use at high latitudes due to poor viewing geometry, resulting in large uncertainties in the derived wind vectors. Can polar-orbiting satellites be used to obtain wind information at high latitudes? The idea has been previously explored with some promising results. The Advanced Very High Resolution Radiometer (AVHRR) was used by Herman (1993) to estimate cloud-drift winds for a few Arctic scenes. When compared to rawinsonde winds, the AVHRR winds were found to have a root-mean-square error of 6 m/s. Herman and Nagle (1994) compared cloud-drift winds from the AVHRR to gradient winds computed with the High resolution InfraRed Sounder (HIRS). The AVHRR winds were found to be comparable to the HIRS gradient winds, with root-mean-square errors less than 5 m/s. Turner and Warren (1989) obtained useful cloud track wind information from AVHRR Global Area Coverage (GAC) data in the Weddell Sea, Antarctica. The manual intervention required in these case studies did not allow for routine production.

In this paper we present an overview of a fully automated methodology for estimating tropospheric motion vectors (wind speed, direction, and height) using the Moderate Resolution Imaging Spectroradiometer (MODIS) on-board the National Aeronautics and Space Administration's (NASA) polar orbiting Terra and Aqua satellites. Orbital issues and retrieval methodology are discussed, and case study results are presented. The case study dataset is used in numerical weather prediction (NWP) model impact studies, where the effect of the MODIS winds on forecasts is assessed

2. Orbital Issues

The wind retrieval methodology builds on the cloud and water vapor feature tracking approach used with geostationary satellites. It is therefore necessary to track features over time in a sequence of images. Statistical analyses of visible, infrared, and water vapor wind datasets from geostationary satellites versus rawinsonde data have shown that the optimal processing intervals are 5 minutes for visible imagery of 1 km resolution, 10 minutes for infrared imagery of 4 km resolution, and 30 minutes for water vapor imagery of 8 km resolution (Velden, 2000). How often can we obtain successive images for wind vectors from a polar-orbiting satellite?

Not surprisingly, the answer depends on the latitude and the number of satellites being considered. Figure 2a shows the frequency of time differences between successive overpasses at a given latitude-longitude point during one 24-hour period with a single satellite (Terra). The points show only those overpasses where the sensor (MODIS) would view the Earth location at an angle of 50 ^{o} or less. At 60^{o} latitude there are two overpasses separated by about 10 hours and 13 hours. No useful wind information can be obtained at this latitude with only one satellite. At 80^{o} there are many views separated by orbital period of 100 minutes but there is still a 13-hour gap each day. For other longitudes the gap will occur earlier or later in the day, so that the entire polar area will be covered by multiple overpasses over the course of a day. Although the 100 minute temporal sampling is significantly longer than the optimal processing intervals for geostationary satellites, in theory wind vectors can be obtained during part of every day for the area poleward of approximately 70^{o} latitude.

Figure 2b shows the coverage with two satellites: Terra and Aqua (orbital characteristics based on current plans for Aqua were used). Temporal gaps of a few hours still exist at the lower latitudes of the polar regions, but at the higher latitudes the temporal coverage is very good. With additional satellites; e.g., the NOAA operational weather satellites with the AVHRR, it would be possible to obtain successive views of a given location within minutes of each other (not shown). Given that geostationary satellites provide reliable wind information equatorward of about 60 ^{o} degrees latitude, global coverage can be obtained if polar-orbiting satellites are used for high-latitude coverage poleward of 60 ^{o}.

The methodology employed for wind vector estimation requires three successive images for wind retrievals. With geostationary satellites the spatial coverage is constant. With a polar-orbiting satellite, the coverage from each successive orbit changes, so wind retrievals can only be done for the area of overlap between successive orbit triplets. For each 200-minute time period (three successive orbits each separated by 100 minutes), wind vectors can be obtained for this area of overlap. The satellite's orbit inclination and swath width determine this overlap region, which for Terra is generally poleward of 70 ^{o} latitude.

An additional orbital issue that must be considered is parallax, which is the apparent position displacement of cloud and water vapor features that results from non-nadir viewing angles. A cloud that is viewed off-nadir will appear to be further from the nadir position than it actually is. The greater the viewing angle, the greater is the displacement. For example, at 500 km from nadir the apparent location of a cloud with a height of 3 km will be approximately 2.1 km further from nadir than its actual position. At a distance of 1000 km from nadir the displacement is 4.5 km. The displacement is not the same from one orbit to the next as the viewing geometry and the actual cloud position change. Appropriate corrections for this viewing geometry are needed, especially in the along-track corners of the overlapping region of the orbits where the errors in wind speed due to parallax are largest.

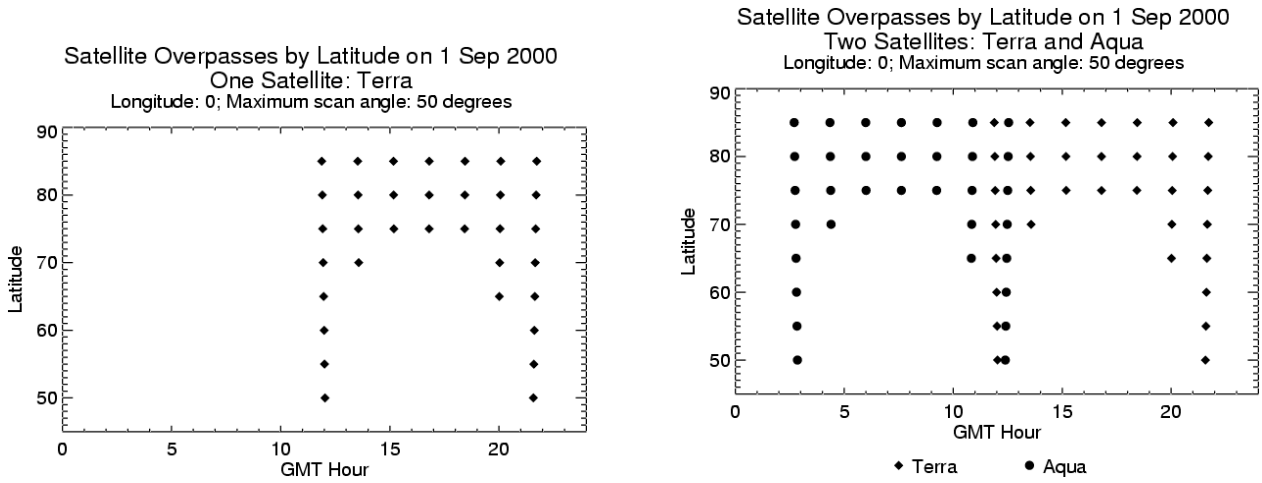

Fig. 2. Time differences between successive overpasses of the Terra satellite (a) as a function of latitude over the course of a 24-hour period at the Prime Meridian, and for both Terra and Aqua (b). Only overpasses with sensor view angles less than 50 degrees are considered.

3. Wind Retrieval Methods

Cloud and water vapor tracking with MODIS data is based on the established procedure used for the GOES, which is essentially that described in Merrill (1989), Nieman et al. (1997), and Velden et al. (1997, 1998). With MODIS, cloud features are tracked in the infrared (IR) window band at 11 μm and water vapor (WV) features are tracked in the 6.7 μm band.

After remapping the orbital data to a polar stereographic projection, potential tracking features are identified. The lowest (coldest) brightness temperature in the infrared window band, generally indicating cloud, within a target box is isolated and local gradients are computed. Gradients that exceed a specified threshold are classified as targets for tracking. For water vapor target selection, local gradients are computed for the area surrounding every pixel rather than the single pixel with the minimum brightness temperature in a box. Water vapor targets are selected in both cloudy and cloud-free regions.

The tracking method searches for the minimum of the sum of squared radiance differences between the target and the search boxes in two subsequent images. A model forecast of the upper level wind is used to provide guidance on the appropriate search area for each target feature. Displacement vectors are derived for each of the two subsequent images. They are then subject to consistency checks to eliminate accelerations that exceed empirically determined tolerances and surface features that may have been misidentified as cloud.

Wind vector heights are assigned by one of two methods. The infrared window method assumes that the mean of the lowest (coldest) brightness temperature values in the target sample is the temperature at the cloud top. This temperature is compared to a numerical forecast of the vertical temperature profile to determine the cloud height. The method is reasonably accurate for opaque clouds, but inaccurate for semitransparent clouds. The choice of the NWP forecast model might have some bearing on the height assignment accuracy. In our case study, the U.S. Navy Operational Global Atmospheric Prediction System (NOGAPS) model with 1.0 degree spatial resolution and 19 vertical levels was used.

The H_2O-intercept method of height determination can be used as an additional metric or in the absence of a CO_2 band. This method examines the linear trend between clusters of clear and cloudy pixel values in water vapor-infrared window brightness temperature space, predicated on the fact that radiances from a single cloud deck for two spectral bands vary linearly with cloud fraction within a pixel. The line connecting the clusters is compared to theoretical calculations of the radiances for different cloud pressures. The intersection of the two gives the cloud height (Szjewach, 1982; Schmetz et al., 1993).

After wind vectors are determined and heights are assigned, the resulting data set is subjected to a rigorous post-processing, quality-control step. A 3-dimensional objective recursive filter is employed to re-evaluate the tropospheric level that best represents the motion vector being traced, to edit out vectors that are in obvious error, and to provide end users with vector quality information (Velden et al., 1998).

4. Atmospheric Considerations

Atmospheric and surface characteristics over polar regions require special consideration in the development of methods for wind retrieval. The polar regions are characterized by low temperatures, ubiquitous atmospheric temperature inversions, low water vapor amounts, bright and cold surfaces, extensive cloudiness, and a high frequency of low, thin clouds. Low-level or surface-based temperature inversions are the rule rather than the exception, even in summer. This is illustrated in Figure 4, which gives standard temperature profiles based on data in Ellingson et al. (1991), and Arctic mean profiles of temperature and humidity that are based on Arctic Ocean coastal and drifting

station data described by Kahl et al. (1992). The Arctic and Antarctic atmospheres are very dry, with total precipitable water amounts of less than 1 cm in the winter and 1-2 cm in summer. Due to the low water vapor amounts, brightness temperature gradients in the 6.7 μm band are small, and surface emission can sometimes contaminate the radiances in clear sky areas. Nevertheless, as will be shown, the water vapor band has proven to be extremely useful in the estimation of polar winds.

Monthly average cloud amounts over the Arctic and Antarctica range from 50-90%, so cloud targets should be numerous. However, the predominant cloud type in the Arctic is marine stratus, with a spatial structure that generally produces fewer tracking features per unit area than other cloud types. A more significant problem occurs with vector height assignment for cloud-drift winds. The H_2O-intercept method is generally not useful for clouds lower in the atmosphere than about 600 hPa because upwelling radiation comes primarily from the atmosphere above the cloud, even in the relatively dry polar atmospheres. The CO_2 slicing method is very sensitive to the clear-cloudy radiance difference, and no height retrievals can be done if that difference is very small. The clear-cloudy radiance differences approach zero as the cloud temperature approaches the surface temperature, as is commonly the case for low clouds. In practice, the CO_2 slicing method is not used for cloud pressures greater (cloud altitudes lower) than about 700 hPa.

Therefore, the infrared window method must be used for low cloud height assignment. With optically thick (opaque) clouds, the IR brightness temperature is a reasonable proxy for the cloud temperature. For thin clouds, the surface and atmosphere below the cloud may contribute significantly to the upwelling radiance. How common are low, thin clouds in the polar regions? Figure 5 shows the relative frequency of cloud pressure and visible cloud optical depth over the Arctic in January and June from the AVHRR Polar Pathfinder (APP) project (cf., Maslanik et al., 2001). Clouds are thin during winter and summer, with the relative frequency of low clouds increasing during the summer. For the Antarctic (not shown) there is also a high frequency of low clouds (relative to the surface elevation). The implication of this for wind retrievals is that low cloud wind tracers need to be treated with caution.

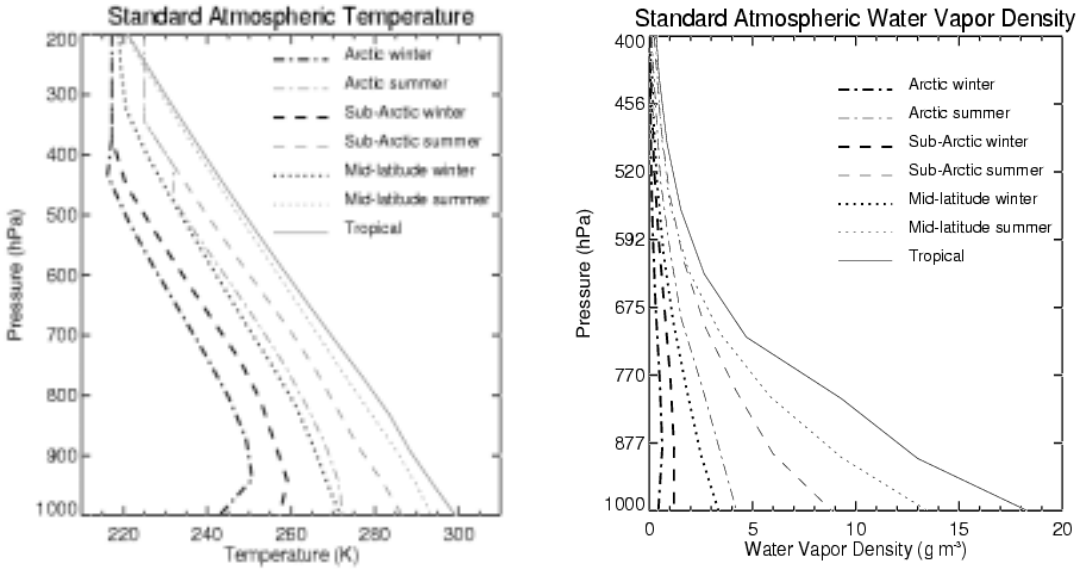

Fig. 4. Temperature (left) and humidity (right) profiles for standard atmospheres and Arctic mean summer and winter.

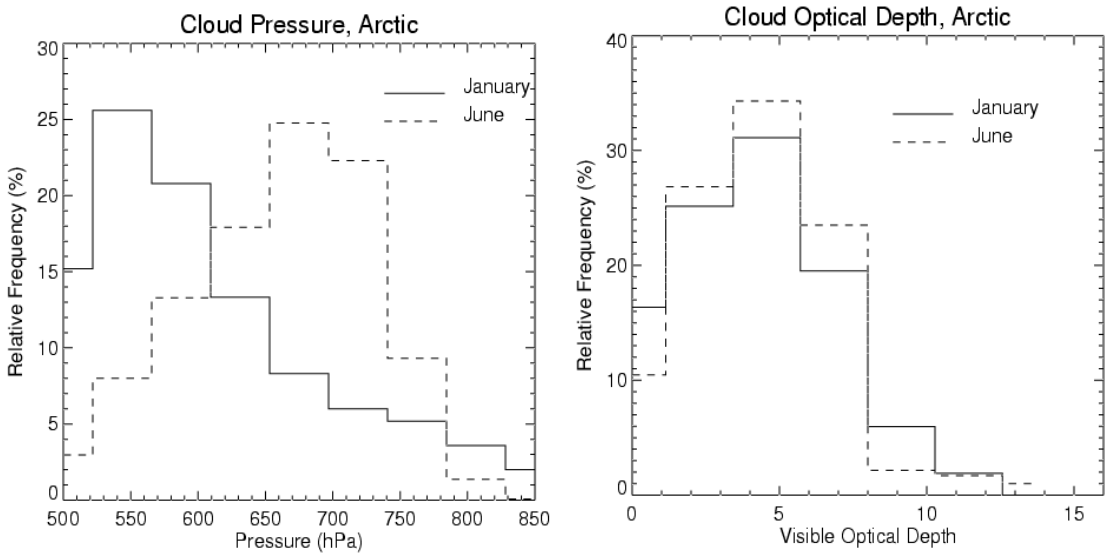

Fig. 5. Relative frequency of satellite-derived cloud top pressure (left) and visible optical depth (right) for January and June in the Arctic. Data are from the extended AVHRR Polar Pathfinder project.

5. Application

A 30-day case study has been completed. The study period is 05 March - 03 April 2001. MODIS Level 1B data from the Terra satellite were acquired from NASA's Goddard Distributed Active Archive Center (DAAC). The 1 km image data were normalized and de-striped to reduce the effect of detector noise and variability. Two to four 5-minute granules from each orbit were remapped into a polar stereographic projection at 2 km resolution and composited with the Man computer Interactive Data Access System (McIDAS). The resulting images are 2800 x 2800 pixels in size. Winds were derived from successive image triplets of the water vapor (band 27) and IR window (band 31) channels. Approximately 25,000 quality-controlled vectors, on average, were produced per day at each pole for the 30-day study period.

Figures 6 and 7 give examples of the wind retrieval results for approximately half of the Arctic. Wind vectors are shown for half of the Arctic study area over a 12-hour period on the first day of the case study. Vectors at all vertical levels are shown, grouped into low (below 700 hPa), middle (400-700 hPa), and high (above 400 hPa) categories. Figure 6 gives the results of IR cloud tracking, where vectors are plotted on the 11 μm image. There are approximately 4,500 vectors in the image with most being in the low and middle height categories. Areas without wind retrievals are, for the most part, clear. Persistently cloudy areas such as the Norwegian Sea will typically have numerous cloud-drift wind vectors. Conversely, areas that are frequently clear, such as Greenland and eastern Antarctica, will have few cloud-drift wind vectors.

Figure 7 gives the results of water vapor tracking, again for a 12-hour period on the first day. Vectors are plotted on the 6.7 μm water vapor image. There are about 13,000 vectors in the image, covering both clear and cloudy areas. In contrast to the cloud-drift wind vectors, the water vapor winds are primarily confined to the middle troposphere. The vast majority of the wind vectors from cloud-drift and water vapor tracking procedures come from the water vapor imagery. This fact certainly reduces the utility of imagers without water vapor channels, such as the AVHRR.

There are two approaches to quantitatively assessing the quality of the wind vectors: comparing the satellite-derived winds with collocated rawinsonde observations, and evaluating their impact on numerical weather prediction. NWP studies are described in the next section. Statistics from comparisons with rawinsondes can provide a measure of product quality over time and can aid in the

determination of observation weights used in objective data assimilation. In the 30-day case study, the root-mean-square (RMS) difference between the satellite winds and rawinsonde observations, averaged over all vertical levels, is 8.11 m/s with a speed bias of –0.58 m/s (satellite wind speed less than rawinsonde) for approximately 27,000 collocations. The RMS differences include errors in rawinsonde measurement and reporting, which are on the order of 3 m/s (Hoehne, 1980). The RMS and bias values are similar to, but slightly larger than, those for geostationary satellite winds. This is expected from the larger temporal sampling intervals. The best results are obtained for the middle and upper troposphere. Low-level RMS differences are larger relative to the mean wind speed for reasons discussed earlier. As Figure 1 illustrates, the verifying observational network is sparse so that these statistics do not necessarily apply uniformly to the entire Arctic and Antarctic.

6. Impact of MODIS Winds on NWP Forecasts

While a polar winds product would be useful for a variety of meteorological and climatological applications, its most important contribution might be in numerical weather predition. Given the sparse rawinsonde observation network in the polar regions (Figure 1), satellite-derived polar wind information has the potential to improve forecasts in polar and sub-polar areas. Model impact studies using the 30-day case study dataset were performed at ECMWF (discussed below) and the NASA Data Assimilation Office (DAO) (Riishojgaard, 2002). The goal for both was to determine if forecasts are improved when MODIS winds are assimilated.

An initial model impact study was performed at the ECMWF with the 30-day case study dataset. All experiments employed a 3D variational analysis assimilation scheme (3DVAR) with 6-hourly analyses that used the model first guess (FG) at the appropriate observation time. The model and analysis resolutions were T159 (approximately 125 km) with 60 levels in the vertical. Ten-day forecasts were run from each 12 UTC analysis.

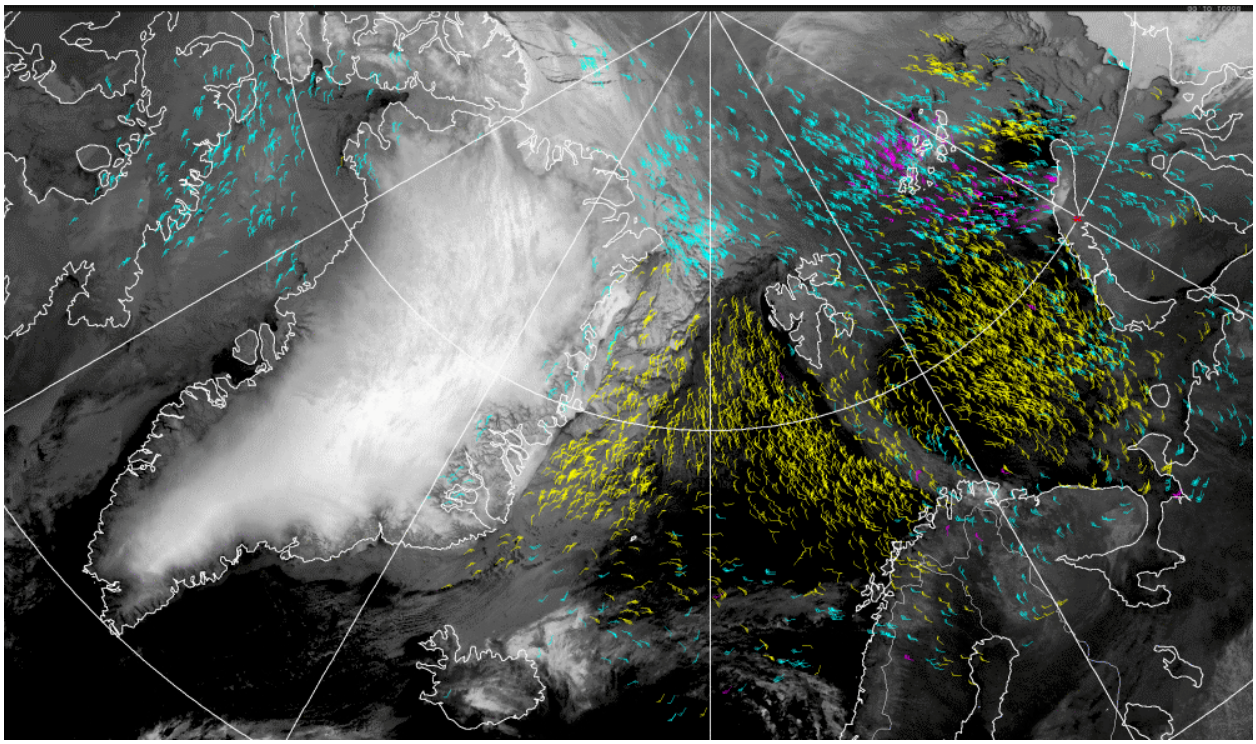

Fig. 6. Cloud-drift winds over the western Arctic from MODIS on 5 March 2001. The wind vectors are overlain on an 11 μm image covering Greenland and the Norwegian Sea. Vector colors indicate the height category: yellow is below 700 hPa, cyan is 700-400 hPa, magenta is above 400 hPa.

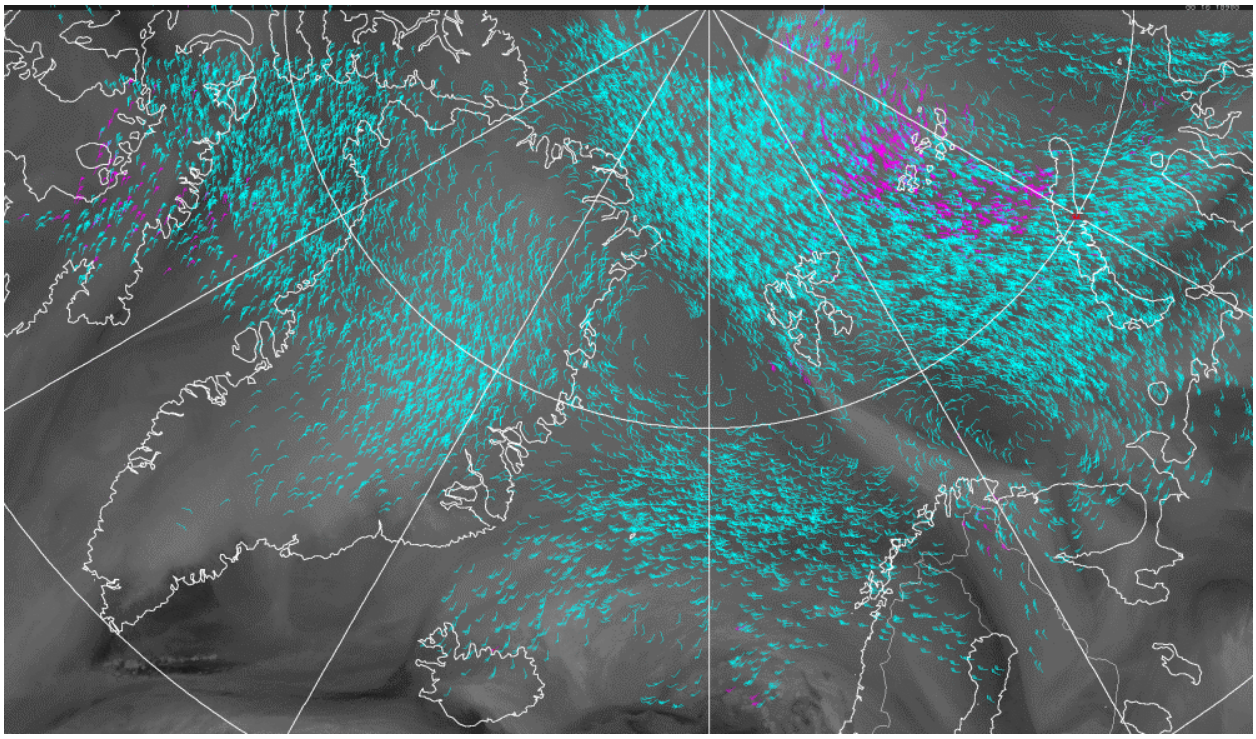

Fig. 7. Water vapor winds over the western Arctic from MODIS on 5 March 2001. The wind vectors are overlain on a 6.7 μm image covering Greenland and the Norwegian Sea. Vector colors indicate the height category: yellow is below 700 hPa, cyan is 700-400 hPa, magenta is above 400 hPa.

Tables 1 and 2 give the first guess statistics from a passive comparison of the MODIS infrared and water vapor cloud winds, respectively, against the first guess used in the assimilation. The tables give the normalized RMS vector difference (NRMSVD), the wind speed bias, the mean wind speed, and the number of cases that were used in the statistics. The NRMSVD is defined as the RMS vector difference divided by the mean wind speed. As with the rawinsonde comparisons, for most levels and regions the NRMSVD and the speed bias are similar to or slightly poorer than other extra-tropical satellite-derived winds currently assimilated by ECMWF. This highlights the acceptable quality of the MODIS winds. The current exception is at lower levels in the Antarctic region where the monitoring statistics reveal large RMS vector errors and relatively strong, fast speed biases (reaching 1.3 m/s). These poorer statistics motivated the cautious use of the MODIS winds at lower levels.

Table 1. First guess statistics for all IR MODIS winds from the control experiment.

	Southern Hemisphere	Northern Hemisphere
Low-level (below 700 hPa)		
NRMSVD	0.64	0.41
Speed bias (observation-FG) (m/s)	1.36	0.54
Mean model speed (m/s)	9.66	12.80
Number of cases	15,319	62,088
Mid-level (400-700 hPa)		
NRMSVD	0.49	0.38
Speed bias (observation-FG) (m/s)	0.56	0.30
Mean model speed (m/s)	14.43	14.70
Number of cases	90,462	78,892
High-level (above 400 hPa)		
NRMSVD	0.40	0.37
Speed bias (observation-FG) (m/s)	-1.38	0.31
Mean model speed (m/s)	21.47	19.49
Number of cases	19,037	3,490

Table 2. First guess statistics for all WV cloud MODIS winds from the control experiment.

	Southern Hemisphere	Northern Hemisphere
Mid-level (400-700 hPa)		
NRMSVD	0.60	0.37
Speed bias (observation-FG) (m/s)	1.39	-0.36
Mean model speed (m/s)	12.55	15.06
Number of cases	282,527	207,324
High-level (above 400 hPa)		
NRMSVD	0.41	0.34
Speed bias (observation-FG) (m/s)	-0.51	0.70
Mean model speed (m/s)	21.29	20.86
Number of cases	80,083	23,196

Globally, the fit of other observations against the first guess or the analysis is not significantly altered when MODIS winds are assimilated. This is also true locally for wind observations from rawinsondes, pilot reports, or aircraft observations for the Arctic region. This lack of change of the first guess fit to other observations suggests that the MODIS winds do not disagree with the rest of the observing network in the Arctic and is thus a positive aspect. Over the Antarctic region, a degradation of the first guess fit against rawinsondes suggests some disagreement between the MODIS winds and rawinsonde winds, at least in the coastal areas where most of the rawinsonde observations are made. As stated earlier, the vertical and horizontal resolution of the forecast fields used in the height assignment for MODIS winds, particularly in temperature inversion regimes, are likely a contributing factor. Future experiments will employ the full resolution ECMWF fields in the data processing.

The mean polar wind analysis is considerably altered in the experiment with MODIS winds. The differences for the Arctic are largest over the sea ice, with differences up to 3 m/s at all levels. Here, the MODIS winds act to strengthen the circulation at upper levels, whereas at lower levels the difference field suggests a weakening of the local circulation. There are some indications that MODIS winds correct deficiencies in the Arctic flow field in the model in this case: the u-component bias between the Canadian Arctic profiler data and the first guess is slightly improved, and the fit of other observations against the first guess is unaltered in the MODIS experiment.

There is a significant positive impact on forecasts of the geopotential heights when MODIS winds are assimilated, particularly over the Northern Hemisphere. Figure 8 shows the improvement in forecasts of the 1000 and 500 hPa geopotential heights over the Arctic (north of 65 ^{o} latitude) when the MODIS winds are assimilated. The figure shows the correlation between the forecast geopotential height anomaly and the verifying analysis with the forecasts from the MODIS and the control experiments each validated against their own verifying analyses. The forecast improvements are significant at the 98% confidence level or better (t-test) at most vertical levels for a forecast range of 2-5 days.

The geopotential height forecast over Antarctica is also improved (not shown) by the inclusion of the MODIS winds, though the impact for the Southern Hemisphere is mainly neutral overall. On the one hand, the less positive impact over the Southern Hemisphere may be related to increased difficulties in the height assignment for the MODIS winds over high and steep orography of the Antarctic continent. On the other hand, verification of forecasts in the Southern Hemisphere is hampered by fewer observations and thus smoother verifying analyses. The addition of MODIS winds is likely to increase the variability of these analyses over the Southern Hemisphere, making an interpretation of forecast scores more difficult. In addition, the synoptic meteorology during our case study period over the Antarctic region was much less active compared to the Arctic, thereby creating less of an opportunity for forecast impact. Further investigations and the use of other verification strategies are required in this respect.

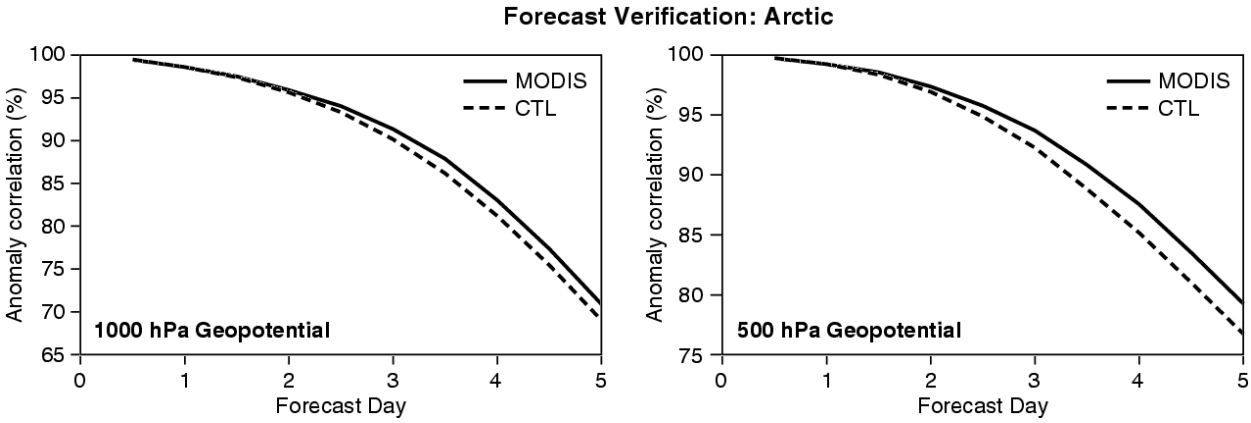

Fig. 8. Anomaly correlation as a function of forecast range for the 1000 hPa (left) and 500 hPa (right) geopotential height forecast in the Arctic region for the ECMWF MODIS winds impact experiments. The MODIS experiment (solid) and the control experiment (dashed) have each been verified against their own analyses. The study period is March 5-29, 2001. The Arctic region is defined as the area north of 65^{o} latitude.

7. Conclusions

This study has demonstrated the feasibility of deriving tropospheric wind information at high latitudes from polar-orbiting satellites. The cloud and water vapor feature tracking methodology is based on the algorithms currently used with geostationary satellites, modified for use with the polar-orbiting MODIS instrument on the Terra and Aqua satellites. Orbital characteristics, low water vapor amounts, a relatively high frequency of thin, low clouds, and complex surface features create some unique challenges for the retrieval of high-latitude winds.

Nevertheless, model impact studies with the MODIS polar winds conducted at ECMWF and the NASA Data Assimilation Office are very encouraging. A 30-day case study dataset was produced and assimilated in the ECMWF model and the DAO assimilation system to assess forecast impact. When the MODIS winds are assimilated, forecasts of the geopotential height for the Arctic, Northern Hemisphere (extratropics), and the Antarctic are improved significantly in both impact studies.

The vast majority of the MODIS polar wind vectors come from tracking features in the water vapor imagery. This fact reduces the utility of imagers without water vapor channels for wind retrieval, such as the current operational NOAA polar-orbiting satellite AVHRR instrument. It also provides strong support for a water vapor channel on the Visible Infrared Imager/Radiometer Suite (VIIRS) that will be flown on the National Polar-Orbiting Operational Environmental Satellite System (NPOESS).

Improvements in height assignment, parallax corrections, and the use of additional spectral channels are under investigation. Progress in any of these areas can be expected to increase the impact of the MODIS polar winds on model forecasts. The impact of these wind data sets should be further enhanced with the use of 4D variational data assimilation techniques. Near real-time processing of MODIS data will begin in the near future, providing a robust dataset for impact studies and meteorological applications. The addition of Aqua MODIS data to Terra MODIS data will allow for even better coverage of the polar regions on a daily basis. . Additional information on this project can be found in Key et al. (2002).

Acknowledgments. This work was supported by NOAA grant NA07EC0676 and NASA grant NAS5-31367.

REFERENCES

Ellingson, R.G., J. Ellis, and S. Fels, 1991, The intercomparison of radiation codes used in climate models: long wave results, *J. Geophys. Res*., 96(D5), 8929-8953.

Herman, L.D., 1993, High frequency satellite cloud motion at high latitudes. *Proceedings of the 8th Symposium on Meteorological Observations and Instrumentation*, Amer. Meteorol. Soc., Anaheim, CA, 17- 22 January, 465-468.

Herman, L.D. And F.W. Nagle, 1994, A comparison of POES satellite derived winds techniques in the Arctic at CIMSS. *Proceedings of the 7th Conference on Satellite Meteorology and Oceanography*, Amer. Meteorol. Soc., Monterey, CA, June 6-10, 444-447.

Hoehne, W.E., 1980, Precision of National Weather Service upper air measurements, NOAA Tech. Memo., NWST&ED-16, 23 pp.

Kahl, J. D., M. C. Serreze, S. Shiotani, S. M. Skony, and R. C. Schnell, 1992, In situ meteorological sounding archives for arctic studies, *Bull. Am. Meteor. Soc*., 73(11):1824-1830.

Key, J. R., David Santek, Christopher S. Velden, Niels Bormann, Jean-Noël Thépaut, Lars Peter Riishojgaard, Yanqiu Zhu, and W. Paul Menzel, 2002, Cloud-drift and water vapor winds from MODIS, *IEEE Trans. Geosci. Remote Sensing*, submitted.

Maslanik, J., J. Key, C. Fowler, T. Nyguyen, X. Wang, 2001, Spatial and temporal variability of surface and cloud properties from satellite data during FIRE-ACE, *J. Geophys. Res*., 106(D14), 15233-15249.

Menzel, W.P., 2001, Cloud tracking with satellite imagery: From the pioneering work of Ted Fujita to the present. *Bull. Amer. Meteorol. Soc*., 82(1), 33-47.

Menzel, W.P., W.L. Smith, and T.R. Stewart, 1983, Improved cloud motion vector and altitude assignment using VAS. *J. Climate Appl. Meteorol*., 22, 377- 384.

Merrill, R., 1989, Advances in the automated production of wind estimates from geostationary satellite imageing. *Proc. Fourth Conf. Satellite Meteorol.*, San Diego, CA, Amer. Meteorol. Soc., 246-249.

Nieman, S.J., W.P. Menzel, C.M. Hayden, D. Gray, S.T. Wanzong, C.S. Velden, and J. Daniels, 1997, Fully automated cloud-drift winds in NESDIS operations. *Bull. Amer. Meteorol. Soc.*, 78(6), 1121-1133.

Schmetz, J., K. Holmlund, J. Hoffman, B. Strauss, B. Mason, V. Gaertner, A. Koch, and L. van de Berg, 1993, Operational cloud motion winds from METEOSAT infrared images. *J. Appl. Meteorol*., 32, 1206- 1225.

Szejwach, G., 1982, Determination of semi-transparent cirrus cloud temperatures from infrared radiances: application to Meteosat, *J. Appl. Meteor.*, 21, 384.

Riishojgaard, L-P., 2002, Impact on MODIS Winds on DAO Systems, *Proceedings of the Sixth International Winds Workshop*, 7-10 May 2002, Madison, Wisconsin.

Rohn, M., G. Kelly, and R. W. Saunders, 2001: Impact of a new cloud motion wind product from METEOSAT on NWP analyses. *Mon. Wea. Rev*., 129, 2392—2403.

Turner, J. and D.E. Warren, 1989, Cloud track winds in the polar regions from sequences of AVHRR images. *Int. J. Remote Sensing*, 10(4), 695-703.

Velden, C.S., C.M. Hayden, S.J. Nieman, W.P. Menzel, S. Wanzong, and J.S. Goerss, 1997, Upper-tropospheric winds derived from geostationary satellite water vapor observations. *Bull. Amer. Meteorol. Soc.*, 78(2), 173-196.

Velden, C.S., T.L. Olander and S. Wanzong, 1998, The impact of multispectral GOES-8 wind information on Atlantic tropical cyclone track forecasts in 1995. Part 1: Dataset methodology, description and case analysis. *Mon. Wea. Rev.*, 126, 1202-1218.

Velden, C.S., D. Stettner and J. Daniels, 2000, Wind vector fields derived from GOES rapid-scan imagery, *Proceedings of the 10th Conf. on Satellite Meteor*., 9-14 January, 2000, Long Beach California, 20-23.